JMEPEG (1996) 5:507-515

Evaluation of the Propensity of Replacements for Halon 1301 to Induce Stress-Corrosion Cracking in Alloys Used in Aircraft Fire-Suppressant Storage and Distribution Systems

M.R. Stoudt, J.L. Fink, and R.E. Ricker

The fire-suppressant agents halon 1301 and halon 1211 have both been determined to possess sufficient ozone layer depletion potential to warrant strict limitations on their production and use. The service conditions aboard jet aircraft subject engine fire-suppressant storage vessels to the agents for long durations at elevated temperatures and pressures. Stress-corrosion cracking (SCC) of the materials of the vessel wall and/or rupture disk assembly (agent release valve) could prevent proper operation. Therefore, the compatibility of potential replacements with the materials used in the fire-suppressant storage and distribution systems is a serious concern.

An evaluation of the relative SCC propensity of 12 halon replacement candidates was conducted to enable the selection of three of these compounds for further study. The slow-strain-rate (SSR) tensile test was selected, and a statistical method was developed for ranking the relative susceptibility of each alloy in each agent from the SSR test results. The results revealed that most agents had little tendency to cause SCC, but that some agent/alloy combinations were undesirable. The statistical technique allowed relative comparison, ranking, and combination of these results with other types of tests for the identification of three agents suitable for development and evaluation as aircraft fire suppressants.

Keywords

bicarbonate cracking, environmentally assisted fracture, halon alternatives, slow strain rate (SSR), stress corrosion cracking (SCC)

1. Introduction

THE ROLE of chlorinated fluorocarbons (CFCs) in the depletion of the ozone layer is of increasing concern. In the proceedings of the 1987 Montreal Protocol (Ref 1), several fully saturated, halogenated compounds were identified as possessing high ozone-depleting potential, thereby resulting in strict limitations on their production and use. Two of the most common fire-suppressant agents, halon 1301 (CF_3Br) and halon 1211 (CF_2Br_2), were included on that list.* Because of their wide range of desirable properties (i.e., no residue after discharge, low toxicity, long-term storage stability, low corrosivity, and low electrical conductivity), these particular chemicals have been the in-flight fire-suppression agents of choice for both engine nacelle and dry bay applications on military and commercial aircraft (Ref 1).

The forthcoming unavailability of these agents has spawned a search for new, environmentally friendly fire suppressants that maintain as many of the aforementioned properties as possible (Ref 1). The results of an examination of the available literature conducted by the U.S. Air Force generated a list of 12 compounds that might be suitable for suppression of fires located inside jet engine nacelles and other aircraft locations. The compounds recommended by the U.S. Air Force for evaluation were HCFC-22 (CHF_2Cl), HCFC-124 ($CHFClCF_3$), HFC-227 (C_3HF_7), HFC-134a (CH_2FCF_3), HFC-236 ($CH_2C_2F_6$), HFC-125 (CHF_2CF_3), HFC-32/HFC-125 azeotrope (CH_2F_2/CHF_2CF_3), FC-31-10 (C_4F_{10}), FC-116 (C_2F_6), FC-218 (C_3F_8), FC-318 (cyclo-C_4F_8), and $NaHCO_3$.

Very little is known about the corrosivity of these chemicals, and there is virtually no information available in the literature regarding the compatibility of these agents with the alloys used for suppressant storage and distribution systems—especially at the temperatures to which they will be exposed in jet engine nacelles (Ref 2). On board an aircraft, metallic components will be exposed to the fire suppressants during storage (e.g., storage vessels, rupture disks, etc.), deployment (e.g., distribution tubes and nozzles), and after deployment (e.g., structural and engine components exposed to combustion by-products). Of these possible exposures, the greatest concern for the safe operation of the aircraft lies in the possibility that the fire suppressant might attack the containment vessels during storage and thereby result in a loss of agent or prevent the proper operation of the deployment system when needed. Therefore, the compatibility of these potential replacements with the wide range of materials used in the agent storage and distribution systems is a serious concern (Ref 3).

According to the U.S. Air Force, aircraft engine fire-suppressant storage bottles typically contain a single agent charge for up to 5 years and are exposed to pressures as high as 5.9 MPa and temperatures ranging from below ambient to 150 °C. Stress-corrosion cracking (SCC) of the materials of the bottle wall and/or rupture disk assembly (agent release valve) could prevent the proper operation of an aircraft engine fire-suppression system. As a result, it was decided that an evaluation of the relative propensity of the 12 compounds to cause SCC of stor-

*Any mention of commercial products in this paper is strictly for informational purposes. It does not imply a recommendation or an endorsement by NIST in any way.

M.R. Stoudt, J.L. Fink, and **R.E. Ricker,** Material Science and Engineering Laboratory, National Institute of Standards and Technology, Gaithersburg, MD 20899, USA, fax (301) 975-4553.

Table 1 Mass fraction of elements in alloys

Alloy	Composition, %														
	Ni	Cr	Mn	Mg	Si	Mo	Nb	N	C	Be	Co	Zn	Cu	Fe	Al
Nitronic 40 SS	7.10	19.75	9.40	...	0.50	...	...	0.29	0.02	...	...	...	...	bal	...
6061-T6 Al	...	0.04	0.15	1.20	0.40	...	...	...	...	...	...	0.25	0.15	0.70	bal
Inconel 625	61.39	21.71	0.08	...	0.09	8.82	3.41	...	0.02	...	...	...	...	3.97	0.23
Type 304 SS	8.26	18.11	1.41	...	0.49	0.17	...	0.03	0.06	...	0.11	...	...	bal	...
CDA-172 Cu-Be	0.06	0.01	...	...	0.08	...	...	...	...	1.90	0.20	...	97.90	0.06	0.04
PH13-8 Mo SS	8.40	12.65	0.02	...	0.04	2.18	...	0.00	0.03	...	...	...	...	bal	1.11
AM-355 SS	4.23	15.28	0.80	...	0.16	2.60	...	0.12	0.12	...	...	...	...	bal	...
AISI 4130	0.08	0.98	0.51	...	0.23	0.16	...	...	0.32	...	...	...	...	bal	0.04

Table 2 As-received heat treatments

Alloy	Mill condition
Nitronic 40 SS	Hot rolled, then annealed
6061-T6 Al	T-6 mill heat treated
Inconel 625	Cold rolled, then annealed
Type 304 SS	Cold rolled, then annealed
CDA-172 Cu-Be	Cold rolled, then tempered 1/4 hard
PH13-8 Mo SS	Hot rolled, then solutionized
AM-355 SS	Solutionized, subzero cooled, then overaged
AISI 4130	Hot rolled

age bottle and rupture disk materials at the temperatures and pressures they are exposed to in the engine nacelle should be included as part of a multifaceted program designed to select three of these compounds for further study and development as an aircraft fire suppressant (Ref 3). To accomplish this objective, a test method that evaluates the SCC resistance of each alloy in each agent and yields numerical results that enable a numerical ranking of relative susceptibility was required. The slow-strain-rate (SSR) tensile test was selected for this purpose, and a statistical method was developed for ranking the relative susceptibility of each alloy in each agent as indicated by the test results. This paper reports the results of this study and ranking of the SCC behavior in the candidate fire suppressants.

2. Experimental Method

Since the objective of this project was to enable the selection of three compounds from the 12 candidates for further development and study as an aircraft fire suppressant, it was decided to evaluate the SCC behavior of the alloys in each agent at 5.9 MPa and 150 °C (Ref 1, 3). The alloys were selected from those currently used for suppressant storage bottles, distribution systems, and rupture disk assemblies or under consideration for future use (Ref 2). The alloys selected for this study were type 304 austenitic stainless steel, PH13-8 Mo stainless steel, AM-355 stainless steel, stainless steel alloy 21-6-9 (Nitronic 40), 4130 alloy steel, Inconel alloy 625, copper/beryllium alloy CDA-172, and aluminum alloy 6061-T6. The compositions and heat treatments of these alloys are presented in Tables 1 and 2, respectively. Samples were machined from each alloy with the rolling direction parallel to the tensile axis (Fig. 1).

Slow-strain-rate tensile tests were selected for the SCC experiments because (1) these tests generate numerical data for all tests, even those where there is no environmental interaction; (2) they yield results in experiments of finite duration (1 to 5 days); (3) the applied stress increases throughout the experiment until mechanical failure occurs, ensuring that SCC threshold stresses or strains have been exceeded; and (4) these tests have proved as reliable as any other test as indicators of SCC susceptibility (Ref 5). In this technique, cylindrical specimens are slowly loaded in tension until failure occurs by either intrinsic mechanical deformation and fracture processes or by an environmentally induced or assisted means (Ref 6). The propensity for each agent to promote environmentally induced failure can be evaluated numerically by comparing the load or strain necessary to cause failure in a reference environment (e.g., argon) to that required to cause failure in the agents under the same conditions (Ref 2, 4, 6). Although other SCC test methods are described in the literature (e.g., direct tension) (Ref 7), these test methods are generally designed around a fixed, initial stress or stress intensity that could be below the critical stress intensity required for crack propagation (i.e., K_{ISCC}). In contrast, the SSR technique features a constantly increasing strain, which results increasing stress and stress intensities. With this technique, failure will occur in each test, with or without the presence of SCC, and will always provide a numerical value that can be used for relative evaluation of a particular alloy/environment combination.

Even though the SSR technique has proved as reliable as any other testing technique for assessing SCC susceptibility, one should keep in mind the limitations of the technique (Ref 5). Since the constant loading and straining conditions of the SSR technique represent loading conditions more severe than most applications, this SCC testing technique also tends to be more severe, and most of the reported errors pertain to the indication of environmental cracking when none is observed in service (false positives). On the other hand, incidents of cracking occurring in service when none was indicated in SSR tests (false negatives) have been reported, but most of these have been attributed to the SSR test environment failing to accurately reflect the actual service environment conditions or strain rates that are too high for the operating cracking mechanism (Ref 5). Crevices can cause local changes in the environment, and the potential of the sample in service may differ significantly from that of the sample in the SSR test, especially since the constant straining also tends to lower the potential of the sample (Ref 5).

Because of the large matrix of alloy/environment combinations to be tested, tests could not be conducted over a matrix of conditions for each combination. As a result, it was decided to conduct tests at a single crosshead speed (2.54×10^{-8} m/s),

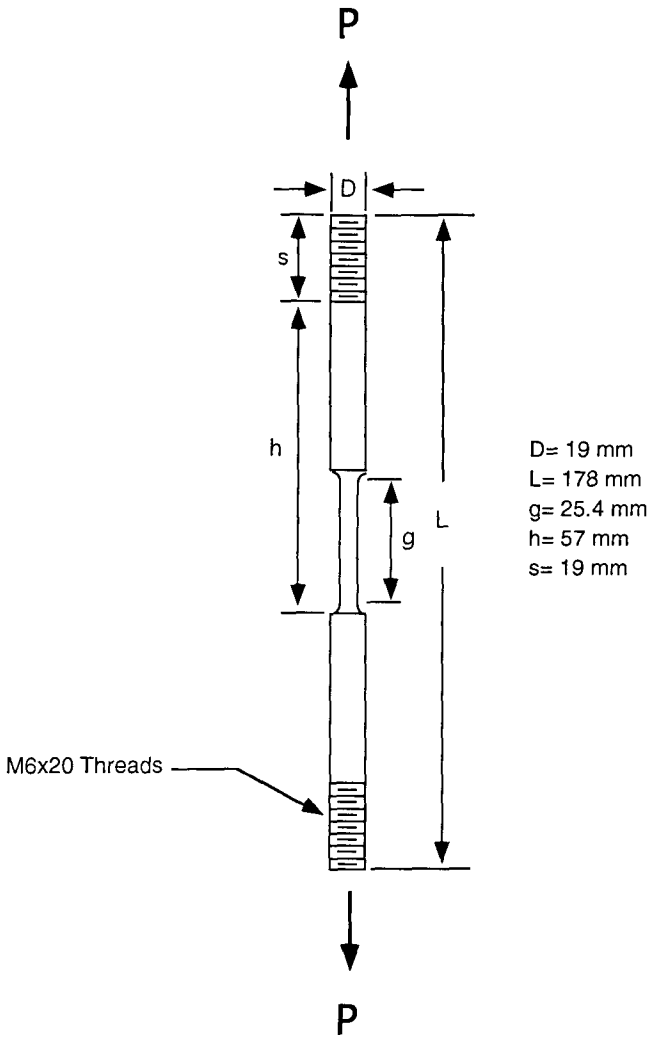

Fig. 1 Slow-strain-rate tensile sample design. Source: Ref 4

which experience has shown usually demonstrates some reduced ductility for environmental conditions that cause cracking. The tests were also conducted under free corrosion conditions (open circuit) because the resistivity of these agents is so high that the samples will be essentially under open-circuit conditions in service (Ref 3, 4).

The tests were conducted in commercially pure agent (i.e., the applicable MIL specifications for impurities were met) (Ref 1). The procedures used for sample preparation and charging are detailed in Ref 3 and 6. The $NaHCO_3$ experiments required a slightly different procedure to accommodate the fluidized powder. For these tests, an appropriate volume of $NaHCO_3$ powder (ball milled to a nominal particle size of 20 μm, with 2 wt% SiO_2 added as a desiccating flow agent) was added to fill the vessel to approximately the midpoint of the gage section in the tensile specimen (approximately 70 g). The vessel was sealed, evacuated, and then backfilled with CO_2 gas. The test vessels used for all experiments were commercially available autoclaves, modified so that a stress could be applied directly to the tensile specimen in situ under the constant environmental conditions of 5.86 ± 0.5 MPa at 150 ± 1 °C. A schematic diagram of the test cell is shown in Fig. 2.

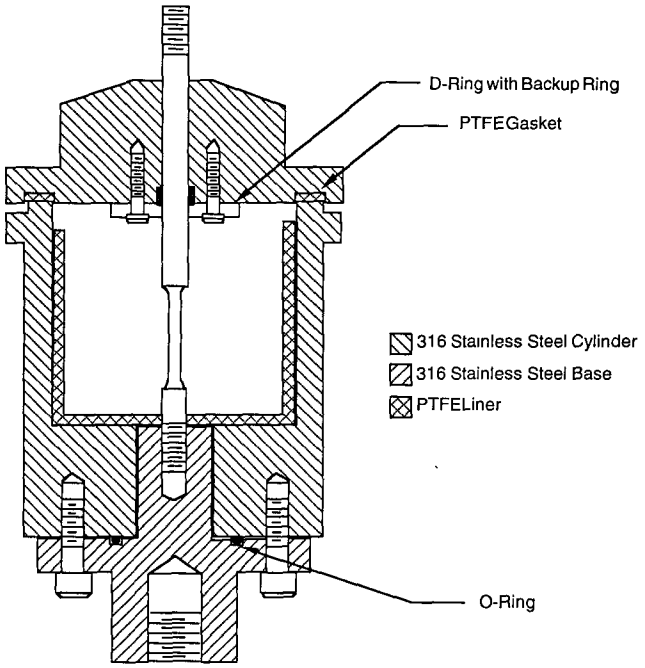

Fig. 2 Slow-strain-rate test chamber

All of the mechanical tests were performed on a computer-controlled SSR testing system that operated at a constant crosshead speed of 2.54×10^{-8} m/s. The computer was configured to sample and record the applied load, the crosshead displacement, and the elapsed time at regular intervals (Ref 4). While the SSR technique is designed to reveal alloy/environment interactions within a reasonable time frame, the duration of an actual test is strongly dependent on the ductility of the alloy. Since each SSR test takes between 40 and 100 h, only the minimum number of tests required for a statistical analysis (i.e., three) could be performed for each alloy in each environment. After failure, the agent was released, the vessels were allowed to cool to ambient temperature, and the samples were extracted from the vessel and stored in a desiccator until analyzed.

The analysis included visual inspections and reduction in area (RA) measurements performed on the fracture surfaces with an optical measuring microscope that had a resolution of $\pm 0.5 \times 10^{-6}$ m. Scanning electron microscopy was later performed on the fracture surfaces of selected samples to verify the presence and/or mode of any cracking. The results of these experiments were then combined and used to formulate a ranking of the potential for failure by SCC for each of the alloys in every replacement candidate.

3. Results and Discussion

3.1 *SSR Data Analysis*

The analysis of the SSR data focused on determining the relative potential for SCC failure in each of the 96 possible alloy/replacement candidate combinations. The susceptibility of a material to environmentally induced failure can be assessed by the two basic parameters measured by a SSR tensile test: ultimate tensile strength (UTS) and ductility. The UTS is deter-

mined from the maximum applied load, and the ductility is commonly determined by two parameters, the engineering strain to failure (STF) and the RA (Ref 8).

The SSR test data were analyzed using two different approaches. The first analysis is based on a ratio between the environment of interest and a reference environment. This is accomplished by calculating the mean values of the UTS, STF, and RA measurements for a given alloy in each agent and then dividing by the mean value for the same alloy tested in the reference environment (argon) at the same temperature and pressure. This mean value ratio (MVR) approach is the technique usually used to interpret SSR test results. Examination of these ratios revealed the alloy/agent combinations where environmentally induced cracking may have occurred. These values are shown in Tables 3 to 5, respectively. They include both the numerical averages of the three tests performed in argon at 150 °C and the values from the tests conducted in laboratory air at ambient temperature.

The UTS is a measurement of the fracture strength of an alloy. A noticeable change should be exhibited in this parameter if some environmental interaction occurs that promotes crack initiation and propagation at lower stresses. Therefore, a significant decrease in the average UTS (Table 3) may be an indication of cracking, but it could also be attributed to corrosion

Table 3 UTS for each alloy tested in argon at 150 °C and ratio for the average UTS in each agent to argon at 150 °C [(mean for agent at 150 °C)/(mean for argon at 150 °C)]

Environment	Nitronic 40 SS	6061-T6 Al	Inconel 625	Type 304 SS	CDA-172 Cu-Be	PH13-8 Mo SS	AM-355 SS	AISI 4130
Argon, MPa	610	240	927	667	874	1136	969	647
Uncertainty(a)	18	26	23	63	24	80	17	46
Ratios								
HCFC-22	0.99	0.97	0.96	1.01	0.98	1.02	0.97	0.96
HCFC-124	1.02	0.98	1.01	0.97	0.98	0.90	0.98	1.03
FC-31-10	1.01	0.98	0.98	0.97	0.96	1.01	0.97	1.04
HFC-227ea	1.00	0.98	0.98	1.00	0.99	1.02	0.96	1.00
HFC-125	1.00	0.98	1.00	0.97	0.97	1.02	0.95	1.03
FC-116	0.98	0.92	0.97	0.96	0.95	1.02	0.95	0.97
HFC-134a	1.01	0.94	1.01	0.98	0.97	1.01	0.96	1.06
HFC-236	1.00	1.02	1.00	0.95	0.99	1.03	0.97	1.00
FC-318	0.98	1.20	1.00	0.83	0.97	1.04	0.98	0.86
FC-218	1.02	0.98	1.02	1.02	0.96	1.03	0.96	1.02
HFC-32/125	1.02	0.94	0.96	0.93	0.96	1.00	0.95	0.97
$NaHCO_3$	1.02	1.05	1.02	0.96	0.98	1.07	0.98	1.04
Alloy avg.	1.00	1.00	0.99	0.96	0.97	1.02	0.97	1.00

(a) The uncertainty is the standard deviation for the alloy and measurement technique as estimated from the variance determined for the measurements in argon and in the agents.

Table 4 Average STF in argon at 150 °C and ratio of the STF in each agent to argon at 150 °C [(mean for agent at 150 °C)/(mean for argon at 150 °C)]

Environment	Nitronic 40 SS	6061-T6 Al	Inconel 625	Type 304 SS	CDA-172 Cu-Be	PH13-8 Mo SS	AM-355 SS	AISI 4130
Argon, %	41.46	7.94	41.03	44.22	10.06	6.21	9.22	7.92
Uncertainty(a)	3.61	1.58	4.56	6.09	1.83	1.04	1.26	0.74
Ratios								
HCFC-22	0.73	1.12	0.92	0.92	1.23	1.20	1.06	1.13
HCFC-124	0.87	1.32	1.06	1.04	1.23	1.28	0.99	1.03
FC-31-10	0.83	1.27	0.91	0.91	1.28	1.05	0.84	1.01
HFC-227ea	0.91	1.34	1.04	1.00	1.17	1.11	1.05	0.97
HFC-125	0.97	1.24	1.06	1.11	1.16	1.08	1.06	1.02
FC-116	0.98	1.21	1.12	1.26	1.21	1.11	0.99	1.12
HFC-134a	0.91	1.19	1.13	0.93	1.00	1.24	1.00	0.99
HFC-236	0.87	1.23	1.01	1.25	0.97	1.13	1.05	1.05
FC-318	1.02	1.07	1.05	0.70	1.27	1.30	0.99	1.20
FC-218	0.99	1.14	1.10	1.11	1.17	1.06	0.97	1.20
HFC-32/125	0.94	1.16	1.13	1.28	1.15	1.16	1.04	1.08
$NaHCO_3$	1.02	0.94	1.12	1.29	1.15	1.70	1.03	0.95
Alloy avg.	0.92	1.19	1.05	1.07	1.17	1.20	1.01	1.06

(a) The uncertainty is the standard deviation for the alloy and measurement technique as estimated from the variance determined for the measurements in argon and in the agents.

reactions that reduced the effective cross section or to a preexisting flaw in the sample. In general, an increase in the average UTS is unusual and may reflect a sample/environment interaction that may be inhibiting deformation and/or fracture. On the other hand, the increases present in Table 3 could merely be the result of interference between corrosion products generated on the sample and the seal of the autoclave through which the sample must slide.

Environmental interactions will generally result in a reduction in the ductility (Ref 2). The majority of the environment/alloy combinations shown in the STF data (Table 4) exhibited increases in the measured strain to failure as compared to the argon values, at the same temperature and pressure. This indicates that deformation may be easier in those agents than in pure argon under the same conditions. It should be noted that the STF values were calculated from load frame displacement measurements taken by a linear variable displacement transducer (LVDT) positioned outside the autoclave during the experiment. As a result, this measurement included both the elastic and plastic deformation components required to induce failure. Ductility determinations based solely on this quantity usually contain larger experimental error (Ref 8).

The second measurement of ductility, the RA value, is determined by a physical measurement of the fracture surface at the completion of the tensile test. Unlike the STF, the RA measurement is based solely on the plastic component of the deformation required for failure and, as a result, the RA is generally a better measure of an environmental interaction for most engineering alloys (Ref 8). In Table 5, it can be seen that the RA values are significantly lower (greater than 10%) in four of the 96 possible alloy/agent combinations: Al-6061 in HCFC-124, Al-6061 in $NaHCO_3$, 304-SS in $NaHCO_3$, and AISI-4130 in $NaHCO_3$. Since three of these four values occurred in the same agent, $NaHCO_3$, it would appear that this agent is reacting with these alloys and may induce SCC in these alloys at 150 °C.

Although the MVR approach can be used to identify interactions between an alloy and a replacement candidate, it does not provide a means for evaluating the statistical significance of the deviations for comparison between alloys and environments. That is, it does not provide a means for ranking the relative susceptibilities from the SSR test results. Therefore, a second analysis was performed on the UTS, STF, and RA data. This analysis consisted of the calculation of Student's *t*-statistic for the significance of the difference between the mean determined in each environment and the mean for the same parameter and alloy tested in argon at the same temperature (Ref 9). This statistic is calculated from the relationship:

$$t = \left\{ \frac{(\bar{y}_{envir} - \bar{y}_{argon})}{\sqrt{\frac{S^2_{envir}}{n_{envir}} + \frac{S^2_{argon}}{n_{argon}}}} \right\} \quad \text{(Eq 1)}$$

where $\bar{y}_{envir}$ is the mean of the tests in the agent at 150 °C, $\bar{y}_{argon}$ is the mean of the tests in argon at 150 °C, S^2_{envir} is the variance of the tests conducted in the agent at 150 °C, S^2_{argon} is the variance of the tests conducted in the argon at 150 °C, n_{envir} is the number of samples tested in the agent at 150 °C, and n_{argon} is the number of samples tested in argon at 150 °C.

Due to the relatively small sample size for each environment (three samples), this statistic was found to be subject to excessive random variations and indications of environmental effects when no supportive evidence could be obtained by other examinations. Examination of the data indicated that this was due, in part, to the statistical variation of the standard deviation for each set of three samples—especially if the standard deviation for argon was at either extreme of the range. To reduce the variations due to sample size in the variances used in Eq 1, an alloy variance, S^2_{alloy}, was determined for each alloy from the

Table 5 Average RA for each alloy tested in argon at 150 °C and ratio of each agent to argon at 150 °C [(mean for agent at 150 °C)/(mean for argon at 150 °C)]

Environment	Nitronic 40 SS	6061-T6 Al	Inconel 625	Type 304 SS	CDA-172 Cu-Be	PH13-8 Mo SS	AM-355 SS	AISI 4130
Argon, %	79.05	42.14	69.63	67.83	34.38	59.62	48.93	50.28
Uncertainty(a)	2.86	2.31	5.41	9.52	7.07	2.62	2.57	2.58
Ratios								
HCFC-22	1.00	0.95	0.94	1.00	1.13	1.03	1.01	1.00
HCFC-124	1.01	0.85	0.94	1.01	1.07	0.94	0.99	0.97
FC-31-10	1.02	0.95	0.92	1.03	1.10	1.02	1.05	0.95
HFC-227ea	1.01	0.93	0.99	1.03	1.26	1.03	1.00	0.96
HFC-125	1.02	0.93	0.97	1.01	1.11	1.04	0.99	0.98
FC-116	1.01	0.98	1.00	1.06	1.18	1.05	0.99	0.98
HFC-134a	1.02	0.93	1.00	1.02	0.91	1.00	1.03	0.99
HFC-236	1.00	0.97	0.94	1.07	0.96	1.01	0.99	0.98
FC-318	1.01	0.97	1.01	1.01	1.06	1.02	0.97	0.99
FC-218	1.09	1.00	1.00	1.04	0.91	1.00	0.97	0.95
HFC-32/125	11.01	0.97	0.96	1.07	1.10	1.04	0.99	1.00
$NaHCO_3$	1.01	0.83	0.98	0.83	0.98	0.97	1.05	0.88
Alloy avg.	1.02	0.94	0.97	1.02	1.06	1.01	1.00	0.97

(a) The uncertainty is the standard deviation for the alloy and measurement technique as estimated from the variance determined for the measurements in argon and in the agents.

average variance observed for the alloy in all of the environments as:

$$S^2_{alloy} = \frac{1}{N_{envir}} \sum_{envir} (S^2_{envir}) \quad \text{(Eq 2)}$$

where N_{envir} is the number of environments. Using this variance in Eq 1 yields:

$$t = \left\{ \frac{(\bar{y}_{envir} - \bar{y}_{argon})}{\sqrt{\frac{n_{envir} - n_{argon}) S^2_{alloy}}{n_{envir} n_{argon}}}} \right\} \quad \text{(Eq 3)}$$

Using this statistic significantly reduced the number of alloy/environment combinations where an environmental effect on ductility was indicated, as shown in Table 6.

The probability of observing the measured difference when there is no environmental influence decreases as the magnitude of the t-statistic in Table 6 increases. The actual probability depends on the degrees of freedom, ν, which is four for these comparisons. The probability of observing a t-value below –0.941 for four degrees of freedom when there is no environmental effect reducing ductility is ≤20%. Fourteen of the 96 alloy/environment combinations (14.6%) had t-values for change in RA that were less than this value. As a result, all of these indications are within the expected range of variations due to normal statistical fluctuations. All of the samples tested in the alloy/environment combinations where $t < -0.941$ were examined fractographically to determine if there was any fractographic evidence of an environmental fracture process. All of the aluminum alloy/environment tests had slightly low t-values. This was determined to be the result of one of the samples tested in argon demonstrating greater ductility than the others, thereby increasing the mean for this environment, but this variation was well within the range of statistical fluctuations. The 4130 steel samples tested in environments with low t-values had some indications of surface corrosion, but no evidence of a change in fracture mode was found. The only alloy/environment where fractographic evidence of an environmental fracture mechanism was observed was one type 304 stainless steel sample tested in $NaHCO_3$.

3.2 *Failure Analysis of Type 304 Stainless Steel*

Fractographic examination revealed that, in general, the $NaHCO_3$ tended to cause more surface corrosion damage—especially in the case of the type 304 stainless steel, where severe cracking was observed on one of the three samples tested in that environment. As a result, the type 304 samples tested in the $NaHCO_3$ were examined in greater detail in order to determine why one sample behaved differently from the other two.

A metallurgical analysis of the type 304 samples revealed that while the samples were purchased to be identical, they were mill processed in two distinctly different manners. Figures 3(a) and (b) are low-magnification optical micrographs of two different type 304 specimens. The microstructure exhib-

Table 6 Student's t-score for the significance of the difference in the means (using RA measurements for each agent and argon at 150 °C)

Environment	Nitronic 40 SS	6061-T6 Al	Inconel 625	Type 304 SS	CDA-172 Cu-Be	PH13-8 Mo SS	AM-355 SS	AISI 4130
HCFC-22	0.09	–1.07	–0.76	0.01	0.66	0.85	0.16	0.07
HCFC-124	0.25	–3.51	–0.76	0.07	0.34	–1.55	–0.27	–0.72
FC-31-10	0.68	–1.18	–1.06	0.29	0.51	0.41	1.16	–1.24
HFC-227ea	0.20	–1.71	–0.13	0.24	1.36	0.69	–0.11	–0.98
HFC-125	0.56	–1.53	–0.45	0.11	0.58	1.02	–0.14	–0.52
FC-116	0.24	–0.56	–0.01	0.51	0.93	1.31	–0.22	–0.51
HFC-134a	0.51	–1.73	0.05	0.15	–0.49	–0.02	0.69	–0.32
HFC-236	0.01	–0.79	–0.76	0.59	–0.23	0.22	–0.14	–0.52
FC-318	0.18	–0.70	0.13	0.10	0.29	0.66	–0.67	–0.34
FC-218	2.95	0.06	–0.06	0.36	–0.45	–0.04	–0.79	–1.26
HFC-32/125	0.18	–0.66	–0.51	0.57	0.53	1.21	–0.18	–0.07
$NaHCO_3$	0.43	–3.87	–0.24	–1.42	–0.09	–0.70	1.19	–2.73
Alloy avg.	0.52	–1.44	–0.38	0.13	0.33	0.34	0.06	–0.76

(a) Due to experimental difficulties, only two tests were run in argon for alloy Inconel 625.

From	To	Frequency Sample SD	Frequency Alloy SD	Interpretation
–∞	–4.60	2	0	Probability of observed difference when no environmentally reduced ductility is less than 0.5%
–4.60	–3.75	1	1	Probability greater than 0.5%, but less than 1.0%
–3.75	–2.78	2	1	Probability greater than 1.0%, but less than 2.5%
–2.78	–2.13	2	1	Probability greater than 2.5%, but less than 5.0%
–2.13	–1.53	7	4	Probability greater than 5.0%, but less than 10%
–1.53	–0.74	13	12	Probability greater than 10%, but less than 25%
–0.74	0.74	44	68	No significant evidence of an environmental effect
0.74	4.60	25	9	Some evidence that the environment enhances ductility

ited in Fig. 3(a) indicates that this material is in a cold-drawn condition (i.e., no annealing after cold working) (Ref 10). In contrast, the much larger, equiaxed grain structure shown in Fig. 3(b) is indicative of a cold-drawn, annealed condition (i.e., an appropriate annealing operation performed after cold working) (Ref 10).

The stress/strain behaviors of the two heat treatments, from tests conducted in argon at 150 °C, are compared in Fig. 4. It can be seen that the yield stress of the material in the cold-drawn condition is on the order of 680 MPa and that the yield stress of the cold-drawn, annealed material is on the order of 550 MPa. Unfortunately, combining these two treatments for all of the type 304 data increased the scatter and the standard deviations determined for this alloy, which made the environmental interaction less obvious in the numerical analysis.

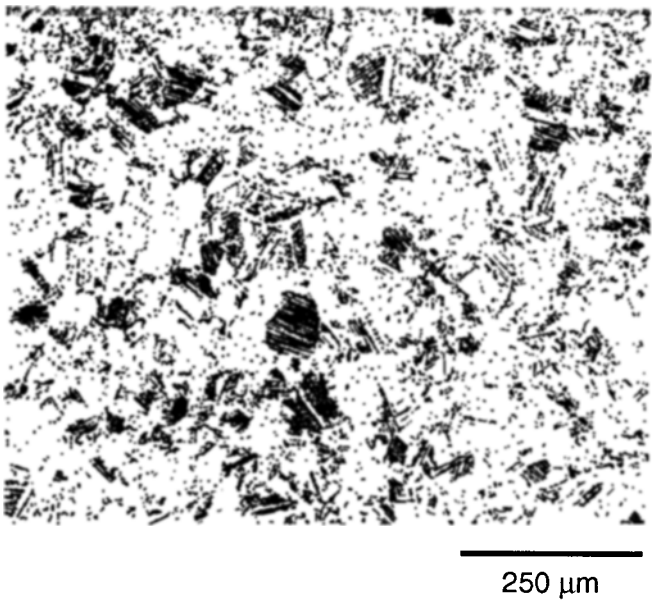

(a)

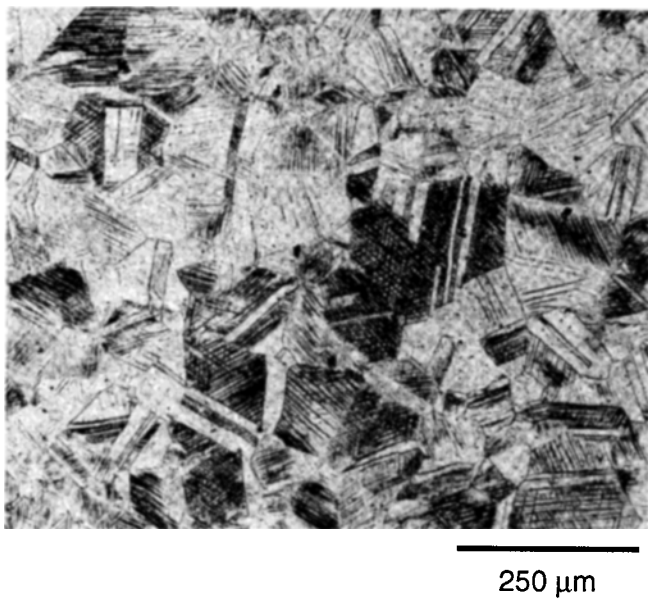

(b)

Fig. 3 Low-magnification optical micrographs of type 304 stainless steel microstructures. (a) Unannealed, cold-worked condition. (b) Fully annealed condition

A review of the literature revealed that, at temperatures between 40 and 80 °C, aqueous $NaHCO_3/Na_2CO_3$ environments may induce cracking in some corrosion-resistant steel alloys (Ref 11, 12) and that some austenitic stainless steel alloys are very susceptible to dealloying in caustic environments at temperatures greater than 100 °C (Ref 11-13). The literature also indicates that the transgranular SCC susceptibility of these alloys is dependent on the nickel content, up to approximately 40% Ni (Ref 13, 14).

Sodium bicarbonate begins a decomposition to sodium carbonate (Na_2CO_3) at 100 °C according to the reaction (Ref 15):

$$2NaHCO_3 \rightarrow 2Na_2CO_3 + H_2O + CO_2 \quad \text{(Eq 4)}$$

Carbon dioxide gas was used to backfill the test vessels in order to substantially increase the partial pressure of CO_2 in the cell and thereby increase the stability of $NaHCO_3$ at 150 °C by suppressing the decomposition reaction. Measurements made on the powder after testing indicated that less than 15% of the bicarbonate had decomposed. However, the sodium carbonate present in the chamber may continue to react with the water generated during the bicarbonate decomposition according to the reaction (Ref 15):

$$Na_2CO_3 + H_2O \rightarrow NaOH + CO_2 \quad \text{(Eq 5)}$$

This reaction is capable of producing small quantities of highly concentrated NaOH, which may then cause a significant shift in the pH over very localized regions on the surface of the sample.

Figures 5(a) and (b) are scanning electron micrographs of the cracking observed on the fracture surface of the type 304 stainless steel specimen tested in $NaHCO_3$ at 150 °C. The overall failure consisted of several relatively shallow, transgranular

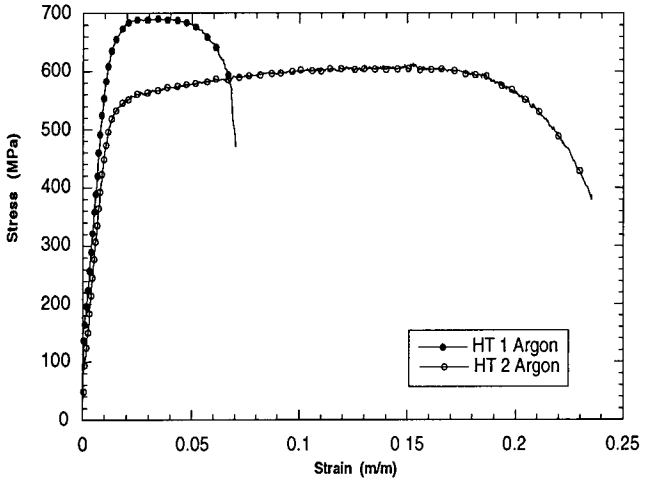

Fig. 4 Comparison of mechanical behaviors exhibited by type 304 stainless steel in the cold-worked and fully annealed conditions

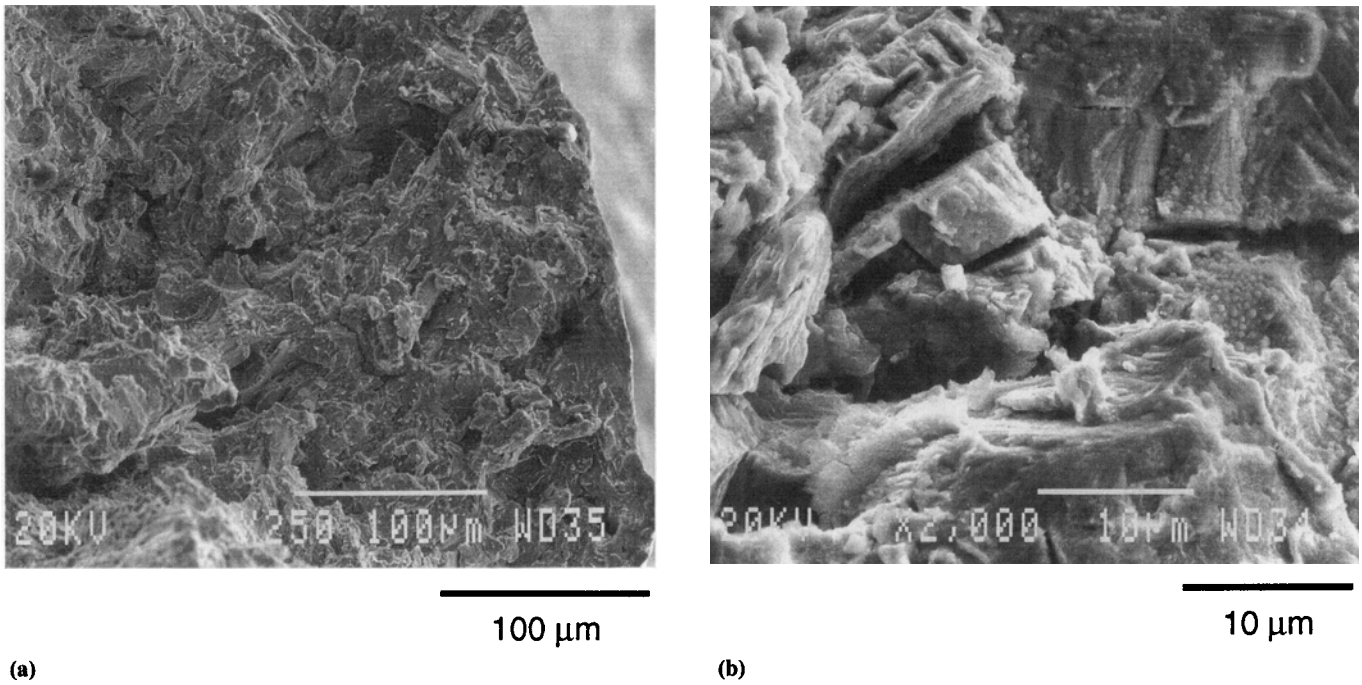

Fig. 5 Scanning electron micrographs of type 304 stainless steel specimen tested in $NaHCO_3$ at 150 °C. (a) Depth of observed cracking. (b) Transgranular cleavage-like crack morphology

cleavage-like (TCL) cracks located along the edges with microvoid coalescence (MVC) in the central region (Ref 16). Figure 5(a), a low-magnification view, shows the depth of penetration observed in a representative crack. The TCL crack morphology is exhibited in the higher-magnification view in Fig. 5(b).

This analysis indicates that the cracking that occurred in one of the three type 304 samples tested in $NaHCO_3$ at 150 °C was the result of (1) a chemical reaction between one or more of the decomposition products of $NaHCO_3$ and the alloy, and/or (2) the metallurgical condition that increased the yield stress, apparently exceeding the threshold stress intensity required for cracking in this environment. While there is not enough information provided by this analysis to conclusively identify the mechanism of cracking observed in this environment, one can speculate about the mechanism involved. Similar TCL cracking has been observed in different alloys and environments and has been attributed to anodic dissolution, hydrogen embrittlement, and film-rupture mechanisms (Ref 13, 17). The experimental technique used to suppress the $NaHCO_3$ decomposition reactions limits the volume of solution that can be generated to quantities that are probably inadequate for an anodic dissolution mechanism (Ref 11, 12). Hydrogen embrittlement is generally observed at temperatures below 100 °C (Ref 13, 17), so it is also an unlikely mechanism for these environmental conditions. This simple analysis indicates that the dealloying-assisted film-induced cleavage mechanism is the most consistent with the observations (Ref 13).

These results clearly illustrate that the prior heat treatment (i.e., annealed, cold worked, quench and tempered) has a significant role in the compatibility between an alloy and a particular agent. In addition, these data also suggest that changes in the heat treatment resulting from the service conditions could dramatically alter the compatibility between the alloy and an agent.

4. Summary and Conclusions

The objective of this study was to select and develop test and analytical methods that would enable the evaluation of the relative potential for SCC failure of fire-suppressant storage containers and rupture disk assemblies in aircraft engine nacelles. Slow-strain-rate tensile tests were selected for these experiments because they generate numerical data for all tests, even those where there is no environmental interaction; they yield results in experiments of finite duration; the applied stress increases throughout the experiment until mechanical failure occurs, ensuring that SCC threshold stresses or strains have been exceeded; and they have proved as reliable as any other test as indicators of SCC susceptibility. None of the agents caused cracking of all the alloys, indicating that any of them could be selected and used. As a result, none of the 12 candidates was rejected from further consideration on the basis of the SCC tests results alone, because at least one storage vessel alloy could be identified for each agent that would not fail by SCC.

The use of mean value ratios for the ultimate tensile strength, strain to failure, and reduction in area data proved sufficient for qualitatively identifying alloy/environment combinations where environmentally induced cracking occurred. However, a quantitative comparison of the relative SCC propensity could not be based on these ratios, because the relationship between the deviation from unity and the probability of the environment influencing the test result is not

the same for the different alloys. To resolve this problem, a statistical technique based on Student's *t*-test for small groups of tests was developed and used to obtain a numerical score for each agent/alloy combination. This numerical score is related to the probability of the observations indicating that the agent influenced the deformation and fracture of the alloy during the tests, making it possible to compare and rank the relative SCC propensity of the agents based on these measurements. This ranking could then be combined with rankings developed from other studies, such as toxicity, fire suppression, and so forth, and used to select three agents for further investigation as aircraft fire suppressants.

It is important to note that the data used in these analyses were obtained from experiments conducted in pure agent on a single heat treatment and at a single temperature and pressure. While this may be sufficient for a preliminary evaluation, a thorough analysis of the influence of alloy heat treatments, impurities in the agent, agent decomposition products, temperature, and strain rate should be conducted on the agents selected for further study before qualifying them for critical applications on aircraft.

References

1. R.G. Gann, J.D. Barnes, S. Davis, J.S. Harris, J.R.H. Harris, J.T. Herron, B.C. Levin, F.I. Mopsik, K.A. Notarianni, M.R. Nyden, M. Paabo, and R.E. Ricker, "Preliminary Screening Procedures and Criteria for Replacements for Halons 1211 and 1301," NIST Technical Note 1278, National Institute of Standards and Technology, 1992
2. R.E. Ricker, M.R. Stoudt, J.F. Dante, J.L. Fink, C.R. Beauchamp, and T.P. Moffat, Corrosion of Metals, *Evaluation of Alternative In-Flight Fire Suppressants for Full Scale Testing in Simulated Aircraft Engine Nacelles and Dry Bays,* NIST Special Publication 861, W.L. Grosshandler, R.G. Gann, and W.M. Pitts, Ed., National Institute of Standards and Technology, 1994
3. W.L. Grosshandler, R.G. Gann, and W.M. Pitts, Ed., *Evaluation of Alternative In-Flight Fire Suppressants for Full Scale Testing in Simulated Aircraft Engine Nacelles and Dry Bays,* NIST Special Publication 861, National Institute of Standards and Technology, 1994
4. M.R. Stoudt and R.E. Ricker, "Characterization of the Hydrogen Induced Cold Cracking Susceptibility at Simulated Weld Zones in HSLA-100 Steel," NIST Internal Report 5408, National Institute of Standards and Technology, 1994
5. J.A. Beavers and G.H. Koch, Limitations of the Slow Strain Rate Test Technique, *Slow Strain Rate Testing for the Evaluation of Environmentally Induced Cracking: Research and Engineering Applications,* STP 1210, R.D. Kane, Ed., ASTM, 1993, p 22-39
6. M.R. Stoudt, J.L. Fink, and R.E. Ricker, "Evaluation of the Stress Corrosion Cracking Susceptibility of Fire Suppressant Storage Container Alloys in Replacement Candidates for Halon 1301," presented at Tri-Service Conference on Corrosion (Orlando, FL), 1994
7. "Standard Practice for Making and Using U-Bend Stress-Corrosion Test Specimens," G 30, *Annual Book of ASTM Standards,* Vol 03.02, ASTM, 1993
8. G.E. Deiter, Mechanical Metallurgy, *McGraw-Hill Series in Materials Science and Engineering,* 3rd ed., M.B. Bever, Ed., McGraw-Hill, 1986, p 275-324
9. W. Mendenhall and T. Sincich, *Statistics for Engineering and the Sciences,* 3rd ed., Dellen Publishing, 1992
10. *Metallography and Microstructures,* Vol 9, *Metals Handbook,* 9th ed., ASM International, 1985
11. R.W. Revie and R.R. Ramsingh, Effects of Potential on Stress-Corrosion Cracking of Grade 483 (X-70) HSLA Line-Pipe Steels, *Can. Metall. Q.,* Vol 22, 1983, p 235-240
12. G.R. Hoey, R.R. Ramsingh, and J.T. Bowker, "Dependence of Stress Corrosion Cracking of Parent, Heat-Affected Zone, and Weld Metal of HSLA Line-Pipe Steel on Potential," presented at Corrosion Monitoring in Industrial Plants Using Nondestructive Testing and Electrochemical Methods (Montreal), 1984
13. R.C. Newman and A. Mehta, "Stress Corrosion Cracking of Austenitic Steels," presented at Environment-Induced Cracking of Metals (Kohler, WI), 1988
14. H.R. Copşon, Effect of Composition on Stress Corrosion Cracking of Some Alloys Containing Nickel, *Physical Metallurgy of Stress Corrosion Fracture,* T.N. Rhodin, Ed., Interscience, 1959, p 247-269
15. M. Windholz, *The Merck Index,* 9th ed., Merck, 1976
16. *Fractography,* Vol 12, *Metals Handbook,* 9th ed., ASM International, 1987
17. A.J. Sedriks, Corrosion of Stainless Steels, *The Corrosion Monograph Series,* R.T. Foley, N. Hackerman, C.V. King, F.L. LaQue, and Z.A. Foroulis, Ed., John Wiley & Sons, 1979